

Alfvén Instability in ITER Baseline Scenario with $I_p=15$ MA

S.E.Sharapov¹ and H.J.C.Oliver²

¹Culham Centre for Fusion Energy, Culham Science Centre, Abingdon, Oxfordshire OX14 3DB, UK

²H H Wills Physics Laboratory, University of Bristol, Royal Fort, Tyndall Avenue, Bristol BS8 1TL, UK

INTRODUCTION

- Burning plasmas in ITER constitute a challenging new field of physics, which requires, in particular, understanding of fundamental issues associated with the super-Alfvénic energy range of fusion-born alpha-particles and ions used in auxiliary NBI heating [1, 2].
- Present-day experiments with NBI and ICRH: fast ion-driven Alfvén instabilities in a broad frequency range, with the effects on fast ion transport ranging from negligible for benign mode saturation to significant for high-amplitude modes (see, e.g., [3] and References therein).
- The ITER scale plasmas with many modes and small ratio between the fast particle orbit and minor radius, $\rho_\alpha/a \approx 10^{-2}$, goes well beyond the present-day experiments. Therefore, extrapolation towards ITER is not straightforward and Alfvén instability remains a significant issue for high-Q operation.
- Since ITER can only tolerate fast particle losses of a few percent, primarily due to first wall damage that they would cause, it is essential that any burning plasma experiment has a window of operation where either the fast ion-driven Alfvén modes are stable, or, if unstable, the effect of instability leads only to a mild rearrangement of the fast-particle distribution.
- The linear instability of Alfvén Eigenmodes (AEs) in the baseline ITER burning plasma scenario with plasma current of $I_p = 15$ MA [4] is considered in this presentation.

ITER ASTRA PROFILES AND EQUILIBRIUM

We consider plasma parameters and profiles predicted with the ASTRA transport code [4] for ITER baseline scenario with current $I_p = 15$ MA, $R_0 = 621$ cm, $a = 200$ cm, and $B_0 = 5.3$ T. The model is based on 2D SPIDER equilibrium for the baseline 2008 separatrix, and the prediction of the plasma profiles is obtained from 1D scaling-based transport for electron and ion temperatures, T_e , T_i , current density, j , electron and ion densities, n_e , n_D , n_T , n_{He} , n_{Be} . The fuel ion species have deuterium-tritium (DT) mixture close to the optimum, $n_D : n_T \approx 50:50$, while density of helium ions resulting from the fusion reactions varies as function of fusion reactivity, and the beryllium impurity ions coming from the first wall satisfy $n_{Be} = 0.02n_e$. The auxiliary heating and current drive includes two deuterium Negative NBI sources with $E_{beam} = 1$ MeV and total power $P_{beam} = 16.5$ MW (on-axis)+16.5 MW (off-axis), and ECRH from the upper launcher has $P_{ECRH} = 6$ MW.

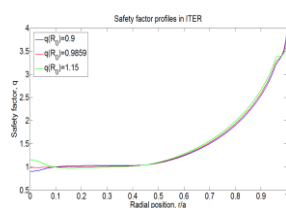


Figure 1. $q(r)$ -profiles considered for the baseline scenario with $I_p=15$ MA.

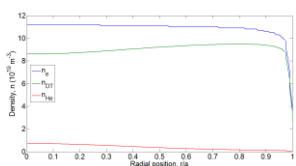


Figure 2. Density profiles of electrons (blue), DT mixture (green), and He (red).

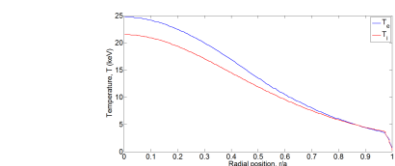


Figure 3. Profiles of electron temperature (blue) and DT ion temperature (red).

Figures 2, 3 show the profiles of densities and temperatures of thermal plasma, for the Q=10 point.

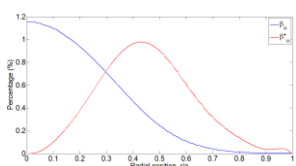


Figure 4. Profiles of $\beta_\alpha(r/a)$ (%) and gradient of alpha-particle pressure, $\beta_\alpha^* = -ad\beta_\alpha/dr$

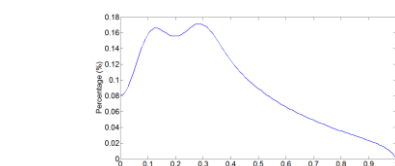


Figure 5. Profile of $\beta_{beam}(r/a)$ (%) in the scenario considered.

Energetic alpha-particle and beam populations shown in Figs.4, 5 are computed within Fokker-Planck approach, and Maxwellian distribution functions are then extracted from the results. Note from Figure 4 that almost all alpha-particles are confined within central region of plasma, $r/a \leq 0.5$, with the highest gradient of the alpha-particle pressure at $r/a \approx 0.42$

STRUCTURE OF TAE AND EAE GAPS

- It is instructive to start the analysis of Alfvén instabilities from investigating radial localisation regions of TAE and EAE gaps, where weakly-damped TAEs and EAEs may reside, for different toroidal and poloidal mode numbers, n and m .
- These localisation points are determined via $q(r_{TAE}) = (m-1/2)/n$ and $q(r_{EAE}) = (m-1)/n$

- The relevant range of the toroidal mode numbers is determined by the efficiency of the alpha particle drive. The maximum power transfer between alpha-particles and an AE is achieved for $n \approx 30$ when drift orbit width of resonant passing alpha-particle, is comparable to the mode width.

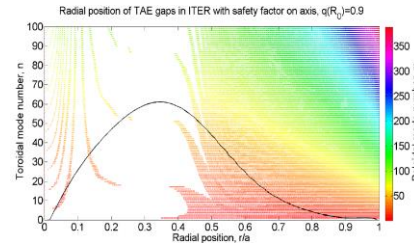


Figure 6. Radial localisation of TAE gaps in ITER with $q(0)=0.9$. Solid line shows normalised radial gradient of alpha-particle pressure. Radial width of a TAE-gap is estimated as $\Delta_{AE} = r/m$.

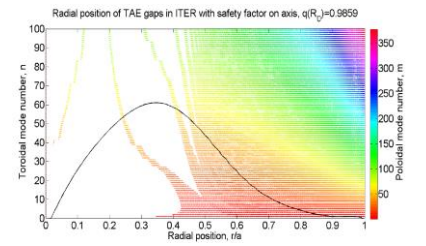


Figure 7. Radial localisation of TAE gaps in ITER case with $q(0)=0.9859$.

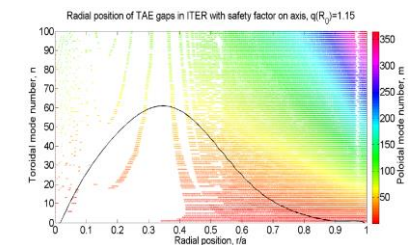


Figure 8. Radial localisation of TAE gaps in ITER case with $q(0)=1.15$.

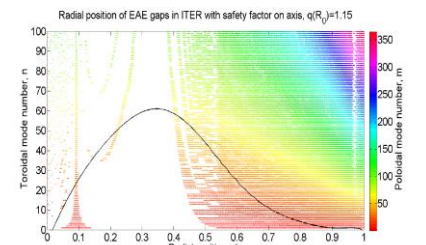


Figure 9. Radial localisation of EAE gaps in ITER case with $q(0)=1.15$.

CORE-LOCALIZED AND GLOBAL MODES AND LOCAL DRIVE/ DAMPING ESTIMATES

In the central region with low magnetic shear, core-localized modes exist as Fig.10 shows. In the region with higher shear values, global modes exist with extended radial width (Fig.11).

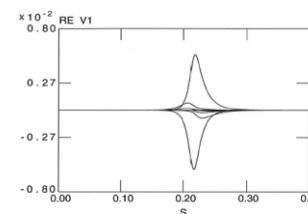


Figure 10. Upper core-localised TAE with $n = 20$ in ITER case with $q(0) = 0.9$.

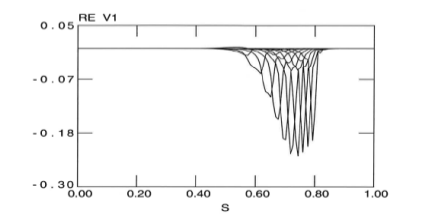


Figure 11. Global TAE with $n = 20$ in ITER case with $q(0) = 0.9$.

Local estimates of TAE drive due to alpha-particles and NBI, together with TAE damping mostly determined by the thermal ion Landau resonance and electron collisions show that TAE instability may occur in the outer plasma region, $r/a > 0.5$.

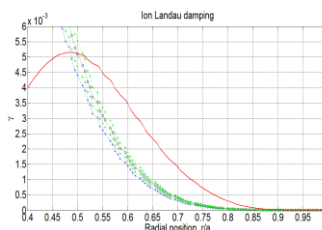


Figure 12. Local Landau damping of TAE due to D and T ions and alpha-particle drive.

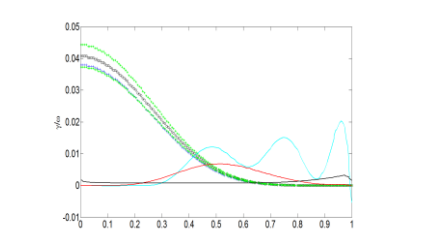


Figure 13. Local Landau damping due to D and T ions, α -drive (red) and NBI drive (blue). Trapped electron damping is shown in black.

CONCLUSIONS

There are two very different regions in the Q=10 ITER operational point with 15 MA:

- 1) $r/a < 0.5$ where main part of alphas is confined, q-profile is flat, and TAE gaps are scarce. In this region, thermal ion Landau damping absolutely dominates over alpha+beam drive;
- 2) $r/a > 0.5$ where alpha-population is not very strong, but TAE-gap density is very high (meaning all TAEs are global). In this region, alpha-drive exceeds the ion Landau damping giving the net drive $\sim 1.5 \times 10^{-3}$. The beam can further destabilise TAEs in this region.

Taking into account the exponential sensitivity of the ion Landau damping to the ion temperature, **the path to the Q=10 point (in the region $T_i < 15$ keV) is likely to be more unstable to TAE than the Q=10 point itself.**

ACKNOWLEDGEMENT

The authors thank S.D.Pinches (ITER Organization) and Ph.W.Lauber (IPP Garching) for providing the transport data for ITER and for important discussions.

[1] ITER Physics Basis, Chapter 5, Nucl. Fusion **39** (1999) 2471.

[2] Fasoli A. et al., *Progress in the ITER Physics Basis*, Chapter 5, Nucl. Fusion **47** (2007) S264.

[3] Sharapov S.E. et al., Nucl. Fusion (2013).

[4] Polevoi A.R. et al., J. Fusion Res. Series **5** (2002) 82.